Evaluation of the attenuation correction on myocardial perfusion imaging: a phantom study

Marisa Machado, Francisco P. M. Oliveira, Lina Vieira, Durval C. Costa

Abstract— **Myocardial perfusion imaging (MPI) with single-photon emission computed tomography (SPECT) is important for risk stratification of coronary artery disease. MPI quantification obtained from available images may not be accurate due to several potential sources of error, being photon attenuation, especially in overweight patients, a significant problem. Attenuation maps derived from X-ray computed tomography (CT) may be used to correct for photon attenuation. The aim of this study was to evaluate the effects of non-attenuation correction (NAC) and attenuation correction (AC) in MPI SPECT imaging using anthropomorphic phantoms simulating patients with different attenuation profiles.**

Forty-nine SPECT and CT studies of Heart/Thorax phantoms with different attenuation layers were acquired. All SPECT imaging data were reconstructed with and without AC. Quantification of the myocardial signal (uptake) was performed in four regions of interest: septum, anterior wall, inferior wall and apex. This was done both in NAC and AC SPECT images. Qualitative evaluation was performed by a nuclear medicine physician also in NAC and AC SPECT images.

The results demonstrated, as expected, statistically lower counts when the thickness of the phantom attenuating material increased and attenuation correction was lacking. On the other hand, when attenuation correction was applied, there were no statistically significant count differences whatever the thickness of the phantom attenuating material. In the qualitative evaluation, the nuclear medicine physician observed small variations in the anterior wall uptake according to the various conditions under test. However, the changes were not statistically significant.

In conclusion, there is no evidence that the effects of attenuation in overweight patients are not properly corrected when the MPI SPECT images are reconstructed with CT-based AC. In terms of qualitative visual assessment, there is no significant variation in the classification of myocardial walls uptake with and without AC when the evaluation is done by an experienced physician.

Index terms- SPECT; attenuation correction; CT; myocardial perfusion imaging; phantom study.

*Research supported by Champalimaud Foundation.

M. Machado is with the Champalimaud Centre for the Unknown, Champalimaud Foundation; and Instituto Superior de Engenharia de Lisboa, Instituto Politécnico de Lisboa (msm225@hotmail.com).

F. P. M. Oliveira is with the Champalimaud Centre for the Unknown, Champalimaud Foundation (francisco.oliveira@fundacaochampalimaud.pt).

L. Vieira is with the H&TRC – Health & Technology Research Center, Escola Superior de Tecnologias da Saúde de Lisboa, Instituto Politécnico de Lisboa (lina.vieira@estesl.ipl.pt).

D. C. Costa is with the Champalimaud Centre for the Unknown, Champalimaud Foundation (durval.costa@fundacaochampalimaud.pt).

I. Introduction

According to the World Health Organization, coronary artery disease (CAD) continues to be the most common cardiovascular disease type and the leading cause of death worldwide [1]. Myocardial perfusion imaging (MPI) with single-photon emission computed tomography (SPECT) is an important technique for risk stratification of CAD [2]. Although MPI SPECT is an important tool to assess myocardial perfusion, the value obtained may not be accurate because there are some sources of error, such as attenuation and Compton diffusion. In order to minimize this degradation, attenuation correction (AC) has been suggested [3]. To correct the attenuation there are several methods that can be used. The one based on attenuation maps derived from X-ray computed tomography (CT) is the most accurate and more often available nowadays. CT-based AC efficiency can be influenced by diverse artifacts such as truncation, error in alignment of CT attenuation maps with SPECT emission data, cardiac motion, and patient-related characteristics [4].

The objective of this study was to evaluate the effects of AC compared to the absence of AC in MPI SPECT studies of patients with different attenuation profiles. Different patients' profiles were simulated using anthropomorphic phantoms.

II. Methodology

The work developed for this project followed a methodology based on anthropomorphic phantoms. The Heart/Thorax Phantom (thorax phantom) and Thorax Overlay (torso overlay) from *RSD, Radiology Support Devices, Inc.* were used. The lungs, heart and liver were included inside the thorax phantom. The heart and liver were filled with ^{99m}Tc diluted in water. The choice of this radionuclide was due to the fact that it is used in the labeling of Tetrofosmin, one of the main radiopharmaceuticals used in MPI studies. When studying the normal biodistribution of ^{99m}Tc-Tetrofosmin in the whole body, Higley B. et al [5] found that 60 minutes after injection, 1.5% of the activity was fixed in the myocardium and 1% in the liver. A standard activity of 9 MBq for the myocardium and 6 MBq for the liver was calculated. The interior of the heart was filled with water only. To simulate a defect, the apex heart region was also filled with water only.

A. *Image acquisition protocol*

Myocardial SPECT studies using the anthropomorphic phantoms were acquired using a two detectors BrightView Gamma Camera (Philips Healthcare, Netherlands, Europe), equipped with low energy and high resolution (LEHR) collimators. After the SPECT acquisitions, CT was acquired

using the CT component of the Gemini TF PET/CT (Philips Healthcare, Netherlands, Europe).

Data collection was performed using two different groups:

- 29 studies acquired with the thorax phantom in supine position;
- 20 studies acquired with the thorax phantom in prone position.

In addition, these 49 studies were subdivided into 5 different acquisition groups:

- 10 acquisitions with the thorax phantom alone and no overlay: 6 acquisitions in supine position and 4 in prone position;
- 10 acquisitions with the thorax phantom + torso overlay: 6 acquisitions in supine position and 4 acquisitions in prone position;
- 10 acquisitions with the thorax phantom + torso overlay + one adipose layer (a fat layer with 1 cm thickness): 6 acquisitions in supine position and 4 acquisitions in prone position;
- 10 acquisitions with the thorax phantom + torso overlay + two adipose layers: 6 acquisitions in supine position and 4 in prone position;
- 9 acquisitions with the thorax phantom + torso overlay + three adipose layers: 5 acquisitions in supine position and 4 acquisitions in prone position (Figure 1).

Figure 1. Positioning of the thorax phantom for acquisition of the CT image in the prone position with torso overlay between the table and the thorax phantom and 3 adipose layers on the top (back of the thorax phantom).

B. Image Reconstruction

After acquisition, SPECT images were processed with a dedicated workstation Extended Brilliance Workspace (EBW) EBW.NM 1.0P v4.0.3.5 2009/07/14 (Philips Healthcare). The process of reconstruction and orientation of SPECT data was performed using the tool package provided by AutoSPECT®Plus software available at the EBW. For the NAC SPECT images reconstruction, we used the optimized OSEM reconstruction algorithm, assuming 2 iterations and 16 subsets, with a Butterworth filter, cut-off frequency of 0.4 cm^{-1}, order 10, and no correction for attenuation.

The AC SPECT reconstructions were performed using AutoSPECT®Plus software, Pro Factory Preferences, General CTAC, using the same reconstruction parameters as before, except that in this case the AC was selected. As the CT images were acquired outside the gamma camera, it was necessary to align the CT images with the NAC SPECT image before the reconstruction with AC. This alignment process was done manually in AutoSPECT®Plus, Pro Factory Preferences.

C. Spatial alignment

To facilitate the comparison of all MPI images (NAC and AC with different attenuation layers), all SPECT images were aligned to each other and with a reference CT using the 3D Slicer 4.8.1 software [6]. Rigid spatial transformations were applied. After the alignment, all SPECT images were resampled for the CT space.

Figure 2 shows an example of the alignment of the SPECT data with the reference CT using 3D Slicer software 4.8.1

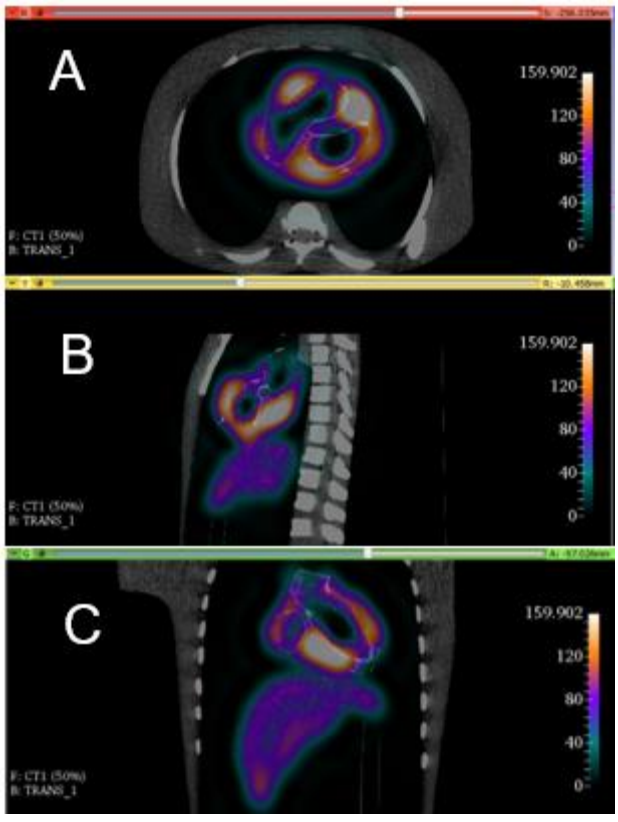

Figure 2. Example of alignment of SPECT images with the reference CT using the 3D Slicer software. (A) transverse plane, (B) sagittal plane and (C) coronal plane.

D. Quantitative analysis

Quantitative data analysis was carried out using 3D Slicer software 4.8.1. Regions of interest (ROI) were drawn

in the reference CT and then transferred to the SPECT studies previously aligned with the CT. Four ROI were considered: septum, anterior wall, inferior wall and apex, as shown in Figure 3.

As quantitative measure, we considered the mean normalized counts (NC) in each ROI. It is given by the mean counts per voxel in each ROI normalized by the acquisition duration (min) and activity (MBq) present in the myocardium at the time of the acquisition (equation 1).

$$\mathrm{NC} = mean\ counts\ /(duration\ \times\ activity) \quad (1)$$

This measure allows comparing the SPECT uptake independently of the duration of the acquisition and the activity in the myocardium.

As the acquisitions were repeated with different attenuation layers, the activity changed from one acquisition to the next. Thus, correction for the decay was always performed according to the decay equation (2), where A is the activity after t hours for the initial activity A_0, and $\lambda = 0.693/6.01$ is the decay constant of ^{99m}Tc.

$$A = A_0 \times e^{-\lambda t} \quad (2)$$

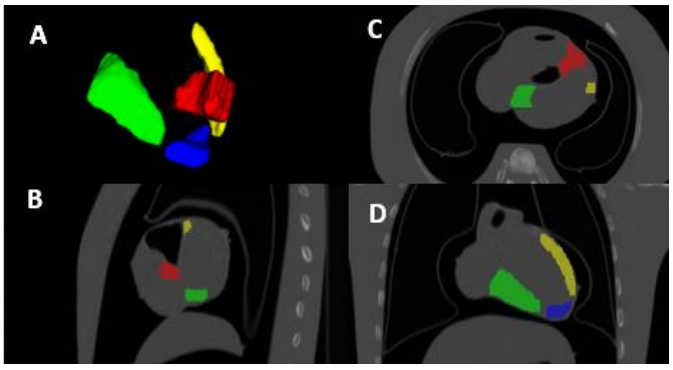

Figure 3. Representation of the anatomical ROIs considered in the phantom. (A) 3D representation of the ROIs, (B) sagittal plane, (C) transverse plane and (D) coronal plane. Septum (red); inferior wall (green); apex (blue); anterior wall (yellow).

E. Qualitative analysis

An experienced nuclear medicine physician carried out a qualitative analysis of all studies. The ROIs considered were visually classified according to four established levels: "no uptake", "normal uptake", "uptake ≤ 50% of the highest myocardial uptake" and "uptake > 50% of the highest myocardial uptake".

F. Statistical analysis

Statistical analysis was carried out on the quantitative and qualitative variables. Both NAC and AC SPECT images were assessed. Friedman statistical test was employed on quantitative variable NC. For the qualitative visual evaluation, the McNemar test was used. Values of $p < 0.05$ were considered statistically significant. All data were analyzed using IBM-SPSS version 20.

III. Results and Discussion

Small uptake variations were observed among the attenuation conditions based on the adipose layers. Thus, only three attenuation thicknesses were considered for the statistical analysis: thorax phantom, thorax phantom + torso overlay, and thorax phantom + torso overlay + 3 adipose layers.

For the NAC SPECT images, a decreasing in the normalized counts in the ROIs with the increasing attenuation layers was observed. For the AC SPECT there was no trend identified. Figure 4 shows the normalized counts in the septum in function of the attenuation layers, for the NAC SPECT (on the top) and AC SPECT (on the bottom). This behavior was entirely similar for the other three ROIs. Friedman statistical test showed no statistically significant differences of the normalized counts in function of the attenuation layers for AC SPECT in all ROIs. On the other hand, statistically significant differences were observed with NAC SPECT images with increasing attenuating thickness in all ROIs (Table 1).

The normalized counts obtained in the apex were very low comparatively to the other ROIs. This was expected since this region was filled only with water. The residual counts were very likely due to partial volume effect from adjacent regions [7-8].

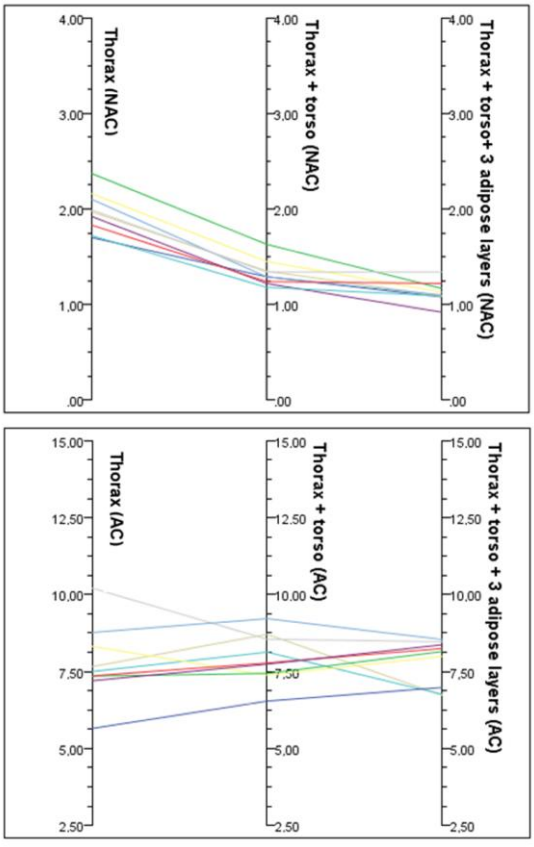

Figure 4. The numbers in the vertical line are normalized counts in the septum for three attenuation conditions. Each line represents an experience (same heart filling) for the three attenuation conditions. On the top, data from NAC SPECT images and on the bottom from AC SPECT images are shown.

The qualitative evaluation presented only variations in the anterior wall. In this region, the physician classified the uptake into two levels ("uptake ≤ 50% of highest myocardial uptake" or "uptake > 50% of highest myocardial uptake"). McNemar statistical test showed no statistical significant differences related to the attenuation layers. The same was true when comparing the visual classification of the anterior wall based on the NAC and AC SPECT images. For all other myocardial regions considered, the qualitative classifications were the same for the NAC and AC SPECT images and for the three attenuation conditions. The septum was always classified as "uptake < 50% of the highest myocardial uptake", the inferior wall as "normal uptake" and the apex as "no uptake".

Relatively to the quantitative variables, the results were as expected. No evidence was found that weight/thickness overload attenuation is not adequately corrected when reconstruction of MPI images is performed with CT-based AC [3, 9].

The results of the qualitative evaluation were concordant with the literature [10-11], since previous studies have reported variations in the anterior wall. In the present work, the differences were not statistically significant. This may be due to the small size of the dataset or the large and long experience of the physician reading the data.

TABLE I. NORMALIZED COUNTS FOR NAC AND AC SPECT INSIDE THE ROI FOR THREE ATTENUATIONS CONDITIONS

Region	**Mean ± standard deviation; median**			***p* value**
	Thorax phantom	***Thorax phantom + torso overlay***	***Thorax phantom + torso overlay + 3 adipose layer***	
Septum (NAC)	2.02±0.25; 1.98	1.34±0.13; 1.32	1.13±0.11; 1.10	< 0.01
Anterior wall (NAC)	1.08±0.13; 1.11	0.76±0.08; 0.75	0.65±0.05; 0.64	< 0.01
Inferior wall (NAC)	1.79±0.17; 1.83	1.30±0.13; 1.32	1.08±0.08; 1.10	< 0.01
Apex (NAC)	0.64±0.18; 0.67	0.47±0.15; 0.50	0.40±0.11; 0.42	< 0.01
Septum (AC)	7.95±1.29; 7.58	7.95±0.76; 7.89	7.80±0.76; 8.15	0.64
Anterior wall (AC)	4.16±0.50; 4.18	4.10±0.47; 4.06	3.88±0.61; 4.01	0.46
Inferior wall (AC)	8.65±0.80; 8.71	8.78±0.65; 8.92	8.52±1.05; 8.82	0.64
Apex (AC)	2.09±0.75; 2.03	1.92±0.36; 1.87	1.97±0.45; 2.02	0.46

IV. CONCLUSION

In this study we found differences in quantification between the MPI SPECT images reconstructed with or without AC for the different attenuation conditions. It was also observed that CT-based AC reconstruction effectively corrects for distortions caused by photon attenuation in the tissues surrounding the myocardium. Thus, if well applied, CT-based AC reduces attenuation artifacts in the MPI SPECT images. However, there are some limitations that prevent the immediate extrapolation of these conclusions to patients. The most important is the utilization of static phantoms, which do not simulate the variability of patients' heart and the movements of the heart.

REFERENCES

[1] WHO, *Hearts: technical package for cardiovascular disease management in primary health care*. Geneva: World Health Organization, 2016.

[2] H. J. Verberne, *et al.*, "EANM procedural guidelines for radionuclide myocardial perfusion imaging with SPECT and SPECT/CT: 2015 revision," *European Journal of Nuclear Medicine and Molecular Imaging,* vol. 42, pp. 1929-1940, November 01 2015.

[3] J. A. Patton and T. G. Turkington, "SPECT/CT physical principles and attenuation correction," *Journal of Nuclear Medicine Technology,* vol. 36, pp. 1-10, 2008.

[4] R. A. Dvorak, *et al.*, "Interpretation of SPECT/CT myocardial perfusion images: common artifacts and quality control techniques," *RadioGraphics,* vol. 31, pp. 2041-2057, 2011.

[5] B. Higley, *et al.*, "Technetium-99m-1,2-bis[bis(2-Ethoxyethyl) Phosphino]Ethane: Human Biodistribution, Dosimetry and Safety of a New Myocardial Perfusion Imaging Agent," *Journal of Nuclear Medicine,* vol. 34, pp. 30-38, 1993.

[6] A. Fedorov, *et al.*, "3D Slicer as an image computing platform for the quantitative imaging network," *Magnetic Resonance Imaging,* vol. 30, pp. 1323-1341, 2012.

[7] R. C. Hendel, *et al.*, "The value and practice of attenuation correction for myocardial perfusion SPECT imaging: a joint position statement from the American Society of Nuclear Cardiology and the Society of Nuclear Medicine," *Journal of Nuclear Medicine,* vol. 43, pp. 273-280, 2002.

[8] T. M. Bateman and S. J. Cullom, "Attenuation correction single-photon emission computed tomography myocardial perfusion imaging," *Seminars in Nuclear Medicine,* vol. 35, pp. 37-51, 2005.

[9] Y. Masood, *et al.*, "Clinical validation of SPECT attenuation correction using x-ray computed tomography–derived attenuation maps: Multicenter clinical trial with angiographic correlation," *Journal of Nuclear Cardiology,* vol. 12, pp. 676-686, 2005.

[10] G. Germano and D. S. Berman, *Clinical Gated Cardiac SPECT*. Malden, Massachusetts: Blackwell, 2006.

[11] M. Tamam, *et al.*, "The value of attenuation correction in hybrid cardiac SPECT/CT on inferior wall according to body mass Index," *World Journal of Nuclear Medicine,* vol. 15, pp. 18-23, 2016.